Available online at www.sciencedirect.com
ScienceDirect
Catena 71 (2007) 444–455
CATENA
www.elsevier.com/locate/catena

Late Holocene paleopedological records contained in tephra from El Chichón volcano, Chiapas, Mexico

Elizabeth Solleiro [a,*], Sergey Sedov [a], José Luis Macías [b], Teresa Pi [a]

[a] Instituto de Geología, Universidad Nacional Autónoma de México, Mexico
[b] Instituto de Geofísica, Universidad Nacional Autónoma de México, Mexico

Abstract

High rates of pedogenesis on unconsolidated volcanic materials imply the accelerated generation of the soil memory. The purpose of this research was to extract the high resolution (centennial scale) paleopedological records from the Late Holocene paleosols of the El Chichón volcano formed during the last 2000 years. We studied buried monogenetic Andosols on the dated tephras and a pedocomplex formed from a set of thin ash layers deposited on older Acrisol derived from shales. Particle size distribution, DCB-extractable Fe, oxalate-extractable Fe, Al and Si, sand and clay mineralogy, organic carbon content and stable C isotope composition in humus were evaluated and interpreted as the elements of the soil memory. However, some differences were found in properties of two buried soils, especially in the kind of A horizons. We attribute such differences of individual Andosols to be caused by ancient human impact because it has been demonstrated that humid conditions persisted during the last 1300 years. Thus the drought that was supposed to provoke the collapse of the Maya civilization at the end of I millennium A.D., should have been a short-term event, below the resolution of this paleopedological record. The Andic Acrisol pedocomplex demonstrated the domination of the humid tropical climate over longer time intervals (probably major part of the Holocene) with possible minor dry episodes.

Keywords: Volcanic paleosols; Chichón volcano; Late Holocene; Pedogenesis; Pedocomplex

1. Introduction

Tephra sediments are isochronous stratigraphic markers that provide an important source of information about volcanic activity in a region. A deposit can accumulate in hours, days, months or even years, followed by periods of quiescence when soil development leaves an imprint on the surface of the sediments. The occurrence of buried soils interlayered with tephra sediments is quite common in volcanic areas all over the world (Campbell, 1986; Frezzotti and Narcisi, 1996; Sedov et al., 2001). Valuable paleoenvironmental records were derived from these sequences, making use of the "soil memory" (in the sense of Targulian and Goryachkin, 2004) of the buried volcanic paleosols. Such records often must be considered semi-continuous, because within the time scale of tephra–paleosol sequences the intervals corresponding to pedogenesis are much longer than those of volcanic sedimentation.

The path ways of pedogenesis in soils derived from such materials are strongly influenced by bioclimatic conditions, and time of exposure to weathering (Ugolini and Dahlgren, 2002). In temperate areas, rates of weathering and soil formation in volcanic ejecta have involved the quantification of neoformed clay, the concentration of aluminum released by acid oxalate (Shoji et al., 1993), mass balances (Jongmans et al., 1993), among others. It has been assumed that transformation of loose volcanic materials (pyroclastics) begins shortly after their deposition and tends to be fairly rapid (Wada, 1985; Shoji et al., 1993; Jongmans, 1994).

We speculate that rapid pedogenesis on the unconsolidated volcanic materials should result in high rates of "soil memory" generation and produce paleopedological records with enhanced temporal resolution. One of the purposes of this work is to extract such a record on the centennial time scale for the Late Holocene from the buried volcanic paleosols of El Chichón volcano (southern Mexico), which has experienced several eruptions during the last 2000 years (Espíndola et al., 2000). These data could clarify the recent environmental history of the tropical Mesoamerica, and in particular — the possible climatic

* Corresponding author.
E-mail address: solleiro@geologia.unam.mx (E. Solleiro).

0341-8162/$ - see front matter © 2007 Published by Elsevier B.V.
doi:10.1016/j.catena.2007.03.012

reasons for the decline of the Mayan civilization (Gill, 1994; Haug et al., 2003). The proxies utilized for paleoenvironmental reconstruction are few and mostly derived from lacustrine records, so additional information from independent sources is required.

The other aim of this research is to interpret from pedogenetic and "soil memory" viewpoints, soil profiles resulting from superimposing volcanic and non-volcanic pedogenesis at different time scales. The periphery of the areas affected by volcanic eruptions is often characterized by deposition of thin ash layers that cover underlying soil profiles and incorporated by the ongoing pedogenesis. This creates a peculiar combination and interaction of the pedogenesis occurring over long time periods, often in non-volcanic parent rocks, and rapid pedogenesis in recently added volcanic materials. The resulting multistory profiles require more study to decipher the soil memory retained within them. The El Chichón volcano area represents a good opportunity to study such profiles because it has a single volcano built upon older sedimentary rocks.

2. Materials and methods

2.1. Physical setting

El Chichón volcano is located at the northwestern margin of the Chiapas state in southern Mexico (Fig. 1). It represents the youngest active volcano of the Chiapanecan Volcanic Arc (Damon and Montesinos, 1978). El Chichón began its formation 0.2 Ma ago and it was reactivated during the Holocene. Locally, the volcano is built upon folded Cretaceous limestones and Tertiary shales and marls (Canul and Rocha, 1981; García-Palomo et al., 2004). El Chichón has erupted at least 12 times during the last 8000 years (Espíndola et al., 2000). The last explosive eruption occurred between March 28 and April 4, 1982. It destroyed 9 towns and killed more than 2000 people (Sigurdsson et al., 1984; Macías et al., 1997) representing the worst volcanic disaster during the modern history of Mexico.

In this work we focus to two Late Holocene paleosols derived from pyroclastic deposits dated at 1250 yr B.P. and 550 yr B.P., studied in detail by Espíndola et al. (2000) and Macías et al. (2003), respectively, and an older soil profile, derived from the shales, and covered by thin ash layers of the Late Holocene eruptions.

The present-day climate is very humid and hot, with 4286 mm-rainfall, distributed during the whole year, and 22.5 °C mean annual temperature. In the areas not affected by the 1982 eruption, the rain forest vegetation is present, with Cedrela, Ceiba and Ficus as dominant species. Over the recent volcanic materials, vegetation is mainly grasses. Soil cover is represented by Leptosols, Chromic Cambisols, Humic Andosols, Chromic Luvisols and Ferric Luvisols.

2.2. Field research and sampling

Two sections were studied at the Chichón volcano (Fig. 2). One, near the town of Volcán (site 1), that was completely buried and abandoned during the 1982 eruption, just 4 km east from the present crater (17°21′59.4″N, 93°11′23.5″W, 675 masl). The second one is located in the outskirts of the town of Chapultenango (17°21′39″N, 93°09′23.7″W, 650 masl), around 10 km east from the crater (site 2). In site 1, two buried soils were found (PCh1 and PCh2), well separated by volcanic materials, constituting monogenetic profiles. In site 2, the same two soils were observed, but there is an additional soil (PCh3), buried by PCh2. In this section, soils are not well separated from each other, and hence, constitute a pedocomplex. The soil formed from the 1982 eruption materials was sampled near the crater (17°21′09″N, 93°13′23.8″W, profile crater), and at site 2. Soils were first classified in the field on the basis of morphological description.

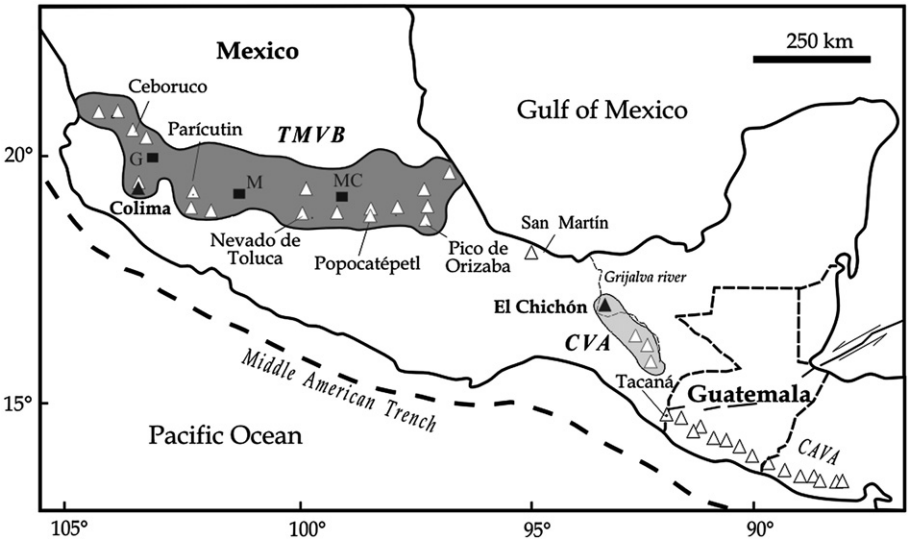

Fig. 1. Map of Mexico showing the Trans-Mexican Volcanic Belt (TMVB) and most important volcanoes. El Chichón is the youngest active volcano of the Chiapanecan Volcanic Arc (CVA) in southeastern Mexico. Abbreviations are: G: Guadalajara; MC: Mexico City; MAT: Middle American Trench; CAVA: Central America Volcanic Arc.

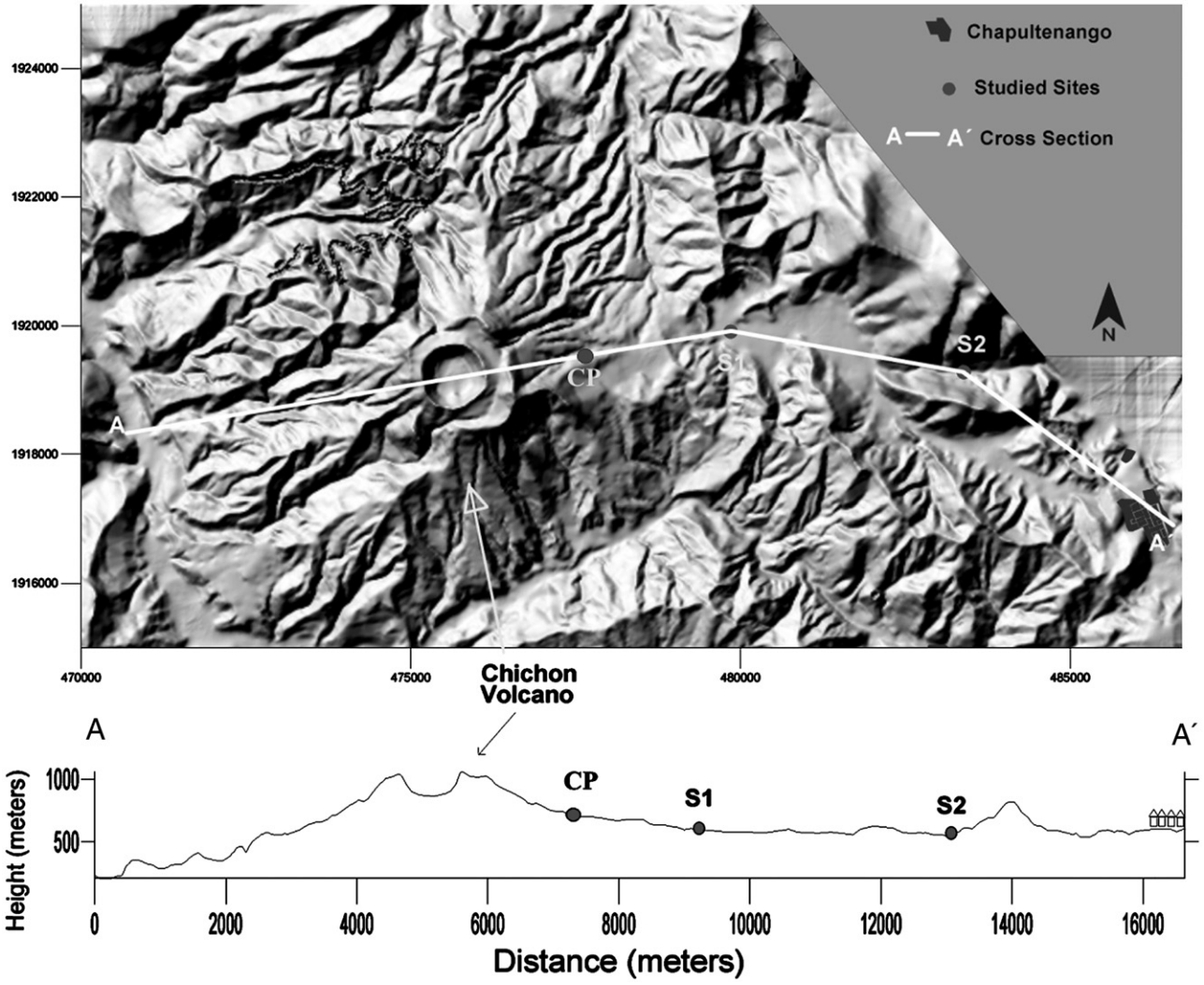

Fig. 2. Digital elevation model of El Chichón volcano that displays the location of study sites. S1—site 1; S2—site 2; CP—crater profile.

Samples for laboratory studies were taken from all genetic horizons of three studied profiles. Besides, we sampled the lowest humus horizon from the site 2 pedocomplex for conventional radiocarbon dating of soil organic matter.

2.3. Laboratory analyses

Selected stable soil properties were evaluated, based on the concept of "soil memory" (Targulian and Goryachkin, 2004) that are useful for pedogenetic analysis and paleoenvironmental reconstructions and not subjected to major diagenetic changes after paleosol burial. The set of such properties for the specific case of volcanic paleosols was defined and interpreted in earlier papers (Sedov et al., 2001, 2003a,b).

Soil colors were determined according to the Munsell Soil Color Charts (2000). Additionally, A horizons of PCh1 and PCh2 were analyzed using a colorimeter for solids CR-310 Minolta, in order to quantify the differences in color. The sand fraction (2–0.02 mm) was separated by sieving; silt (0.02–0.002) and clay (<0.002 mm) fractions by gravity sedimentation with a preliminary destruction of aggregating agents: H_2O_2 (15%) was used to destroy organic matter, dithionite–citrate–bicarbonate (DCB) extraction for iron oxides (no carbonates are present in the studied soils). The particle size fractions were separated quantitatively and the texture was established on the basis of the weight of the fraction separates. Fe, Al and Si, extracted with DCB, oxalate and pyrophosphate solutions, pH in water and pH in NaF were evaluated according to USDA (1996). Organic carbon and total nitrogen were determined using a CHNS/O analyzer, PerkinElmer 2400, series II.

Mineralogical research was carried out on particle size fractions from selected horizons, so that each subprofile is represented by one sample from an A horizon and one or more samples from the middle or lower parts of the profile. Sand mineralogy was studied under a petrographic microscope using the immersion method for the specimens with a liquid having a refractive index of 1.544 (corresponding to Np of quartz). The identification of mineral grains was based on standard crystallographic characteristics. To distinguish quartz from intermediate plagioclase that is abundant in the parent rocks of the area (which have a similar refractive index), in cases where no twinning, cleavage fractures or specific secondary products

Fig. 3. Vitric Regosol formed from 1982 ash, at crater profile.

were observed, we always used interference figures. More than 250 grains were counted in all samples. Mineralogical composition of the clay fraction was studied in selected horizons of all profiles. Clay minerals were identified through X-ray diffraction, employing CuKα-radiation in a Philips diffractometer Mod. 1130/96. Oriented specimens of clay saturated with Mg were prepared. X-ray diffraction patterns of the Mg-saturated clay were obtained for oriented specimens after the following pretreatments: air dry at room temperature, saturated with ethylene glycol, after heating at 400 °C and 550 °C for 1 h.

The carbon-13 content of the soil organic material in modern and buried A horizons was determined by using a combustion method slightly modified from that described by Sofer (1980). The modification consists of the addition of metallic copper Cu^0 to eliminate the NO_2 (Mook and Jongsma, 1987). The time frame for soil formation was established according to the tephrostratigraphy of the area, developed by Espíndola et al. (2000) and Macías et al. (2003). Humus of A horizon in PCh3 was dated by radiocarbon in the Arizona Radiocarbon Laboratory.

3. Results

3.1. Soil morphology, classification, correlation and dating

The crater soil profile is poorly developed and contains an O horizon, 1 cm thick, directly overlying stratified fresh 1982 tephra. The profile was classified as Vitric Regosol (Fig. 3).

In site 1, the PCh1 paleosol, formed from a pumice fall deposit dated at 550 yr B.P., which was buried by 120 cm of ash deposited during the 1982 eruption, contains a 2Ab1, 2Bwb1, 2BCb1, 2Cb1 profile (Fig. 4A). The 2Ab1 horizon (20 cm depth), is brown (7Y 4/2, dry) with a reflectance of 13.25%. It has a very well developed granular structure, and a sandy-clay

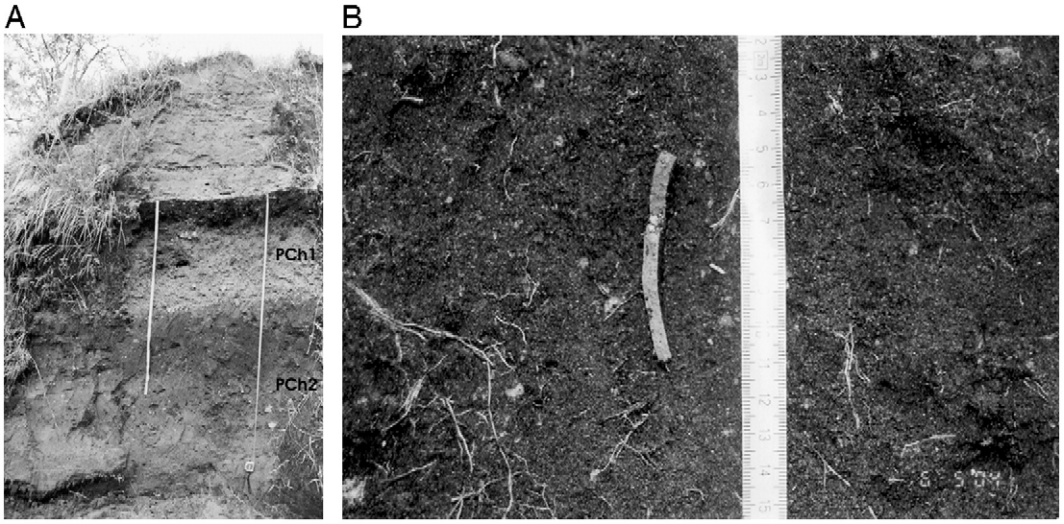

Fig. 4. A) Buried paleosols in site 1: PCh1 and PCh2 showing differences in A horizons. B). A detail of PCh2 showing the rest of prehispanic ceramic.

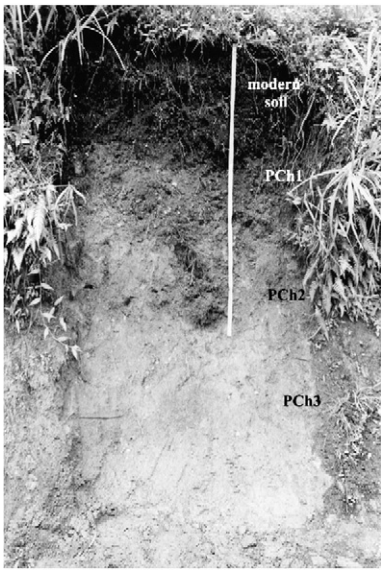

Fig. 5. Buried paleosols in site 2: thin modern soil, PCh1, PCh2 and PCh3 constituting a pedocomplex.

texture. Its lower boundary is gradual and wavy. 2Bb1 horizon is yellow, 25 cm thick, with a subangular blocky structure and is more clayey than the previous horizon. Sand particles are covered by yellow-brown (10YR 4/4) clay. Its boundary with the BC horizon (35 cm thick) is diffuse and gradual. The 2BCb1 horizon is pale yellow (2.5Y 8/4, dry), sandy, with a big quantity of pumice. Structure is massive. The boundary with 2Cb1 horizon is clear. This horizon is composed of a yellow pumice (2.5Y 8/5) fall deposit, of well sorted, coarse ash particles.

The following soil unit (PCh2) was buried by the 550 yr pyroclastic fall and formed from another pyroclastic flow dated at 1250 yr B.P. The profile consists of 3Ab2, 3ABb2, 3BCb2 and 3Cb2 horizons (Fig. 4A). The uppermost horizon (3Ab2), 25 cm thick, has a gray color (1.9Y 5/1.4, dry) and a silty-sand texture. Structure is subangular blocky that breaks into small granules. Boundary with 3ABb2 horizon (20 cm) is gradual, showing similar characteristics but is more sandy. 3Bb2 horizon (20 cm) is light yellowish brown (2.5Y 6/4) with a less developed subangular blocky structure. There is no evidence of clay segregation. Mineral particles are clean. The quantity of gravel is very high. 3Cb2 horizon is a pyroclastic flow (60 cm thick). Artifacts are very common inside this soil (Fig. 4B).

Both PCh1 and PCh2 paleosols are classified as Andosols.

In Chapultenango, site 2, PCh1 consists of a 2Ab1, 2ABb1, 2BCb1, 2Cb1 profile (Fig. 5). The buried profile is separated from the present-day surface by a 12 cm thick modern soil, consisting of A and C horizons. The buried 2Ab1 horizon is 23 cm thick. It has a dark grayish brown color (2.4Y 4/2, dry) with a hard granular structure and a loam texture. The 2ABb1 horizon is grayish brown (Table 1) with a hard subangular blocky structure. The 2BCb1 horizon is yellowish brown, more sandy, less structured with high quantities of pumice. Mineral grains show coatings of clay and iron oxides. This horizon has a mixture of fresh volcanic material, weathered minerals and reworked materials from the underlying horizon.

Table 1
Selected physical and chemical characteristics of soils from this study

Soil	Horizon	Depth (cm)	Color, dry	Color, moist	Reflectance (%)	pH NaF	TOC (%)	TN (%)	C/N	$\delta^{13}C$ (‰)
Profile crater										
Modern	A	0–1	10YR 7/4	10YR 5/4		8.00	3.23	0.29	11.14	
Modern	C	>1	5Y 6/2	5Y 5/3		8.90	0.15	0.12	1.25	
Profile S1										
PCh1	2Ab1	120–140	0.7Y 4.2/1.1 [a]	3.4YR 3.2/0.5 [a]	13.25	10.10	3.61	0.41	8.80	−25.16
PCh1	2Bb1	146–175	10YR 7/4	10YR 5/4		10.20	0.71	0.13	5.46	
PCh1	2BCb1	175–210	2.5Y 8/4	2.5Y 6/4		9.60	0.36	0.09	4.00	
PCh2	3Ab2	210–235	1.9Y 4.7/1.4 [a]	6.2YR 3.3/0.6 [a]	16.65	10.20	1.45	0.18	8.06	−24.54
PCh2	3ABb2	235–255	2.5Y 5/3	2.5Y 3/2		10.30	1.37	0.21	6.52	−24.54
PCh2	3Bb2	255–275	2.5Y 6/4	2.5Y 3/3		10.20	0.84	0.17	4.94	
PCh2	3Cb2	275–335	2.5Y 6/3	2.5Y 3/2		9.50	0.21	0.09	2.33	
Profile S2										
Modern	A	0–3	2.5Y 4/1	2.5Y 3/1		7.90	3.81	0.37	10.30	−18.29
Modern	C	3–12	2.5Y 5/4	2.5Y 4/4		8.20	0.74	0.14	5.29	
PCh1	2Ab1	12–35	2.5Y 4/2	2.5Y 2.5/1		10.00	5.70	0.54	10.56	−21.41
PCh1	2ABb1	35–56	2.5Y 4/3	2.5Y 2.5/1		10.30	3.69	0.39	9.46	−26.90
PCh1	2BCb1	56–100	2.5Y 6/4	2.5Y 5/6		9.70	0.72	0.17	4.24	
PCh2	3Bb2	100–136	10YR 5/4	10YR 3/3		10.10	2.75	0.35	7.86	
PCh2	3BCb2	136–160	10YR 5/4	10YR 3/3		10.40	2.30	0.31	7.42	
PCh3	4Ab3	160–200	2.5Y 6/4	2.5Y 3/2		10.10	3.70	0.38	9.74	−19.79
PCh3	4EBb3	200–242	10YR 6/6	10YR 6/3		9.50	1.93	0.24	8.04	
PCh3	4Bb3	242–257	5YR 6/6	5YR 4/6		8.90	0.75	0.17	4.41	
PCh3	4BCb3	292–352	5YR 6/6	5YR 4/6		8.90	0.54	0.19	2.84	
PCh3	4Cb3	>352	5YR 6/3	5YR 4/6		8.90	0.35	0.21	1.67	

TOC: total organic carbon; TN: total nitrogen; C/N: carbon/nitrogen ratio.

[a] Colors were evaluated using a colorimeter (Chroma Meter CR-310) as well as reflectance.

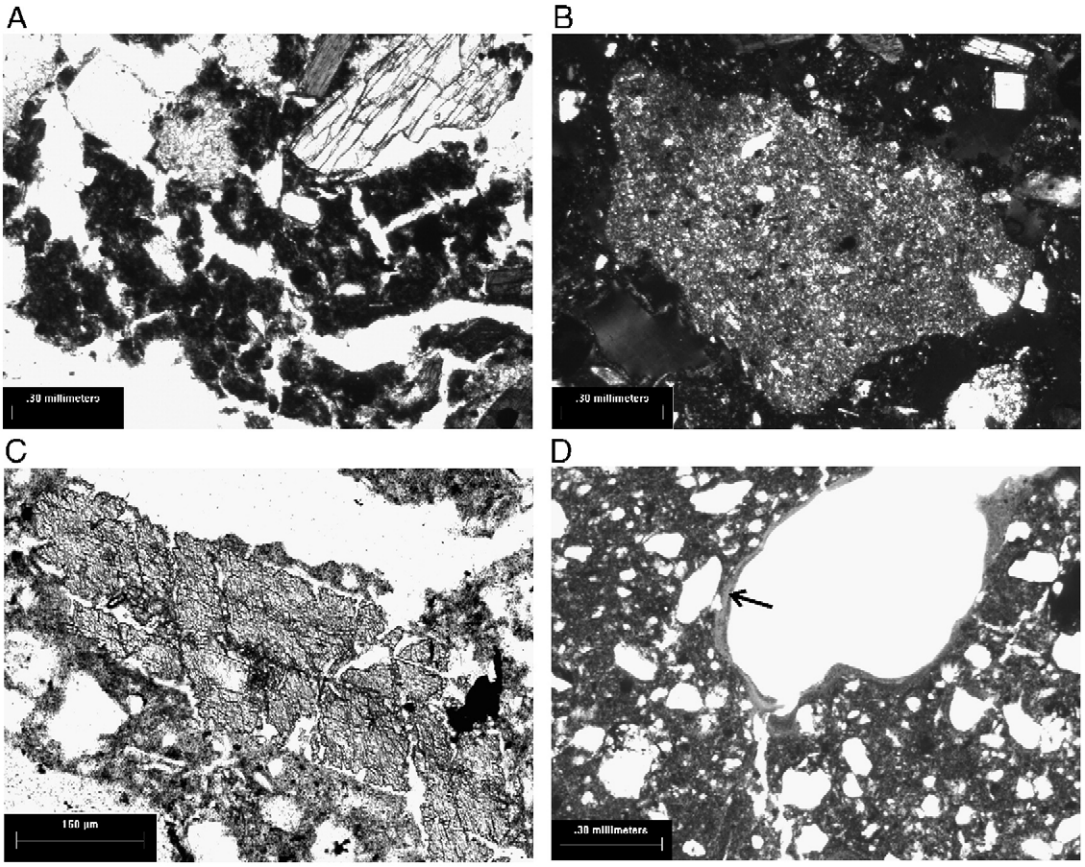

Fig. 6. Micromorphological features of Chichon paleosols. A. Complex structure: deformed granules welded into subangular blocks, 2Ab1 horizon, site 1, PPL. B. Clayey fragment with speckled b-fabric, 3Ab2 horizon, site 1, N+. C. Etched amphibole, 4BCb3 horizon, site 2, PPL. D. Thin clay coatings without lamination in 2BCb1, site 2. Arrow points to a coating, PPL.

PCh2 underlies 2BCb1, but is partly decapitated by erosion and is only constituted by a 3Bb2, 3BCb2 profile. The 3Bb2 horizon (36 cm thick) is yellowish brown (10YR 5/4, dry) with a very well developed subangular blocky structure. It is more clayey and has abundant weathered volcanic rock gravels, as well as shale fragments. The lowermost horizon of this soil is a 3BCb2 (14 cm) lighter in color, clayey with high amounts of gravels of volcanic and shale rocks.

In this section, we found another buried paleosol with a 4Ab3, 4EBb3, 4Bb3, 4BCb3, 4Cb3 profile. 4Ab3 horizon (40 cm) is yellowish brown (2.5Y 6/4, dry), clayey but with a big proportion of sand particles. Structure is well developed subangular blocky. It is very porous. The 4EBb3 horizon (42 cm thick) is lighter in color. The boundary with the previous horizon has weathered volcanic fragments. It also has shale gravels; structure is also in subangular blocks, porous, with clay infillings in channels. The 4Bb3, is reddish yellow (5YR 6/4, dry), 50 cm thick, clayey, with a similar structure as the previous one, but in this case it is better developed, more sticky and compact. There are a few clay cutans. The underlying 4BCb3 horizon (60 cm thick), has clay material in fractures between strongly weathered shale. The parent material of this soil corresponds to shale. It is grayish brown-green, with red spots and Mn segregation, non-structured, but already with a high grade of weathering. The paleosol presented by the b3 subprofile of the pedocomplex was named PCh3 (Fig. 5).

Although the site 2 profile is polycyclic and consists of several superimposed individual subprofiles, we classified it as a whole as Andic Acrisol.

The conventional radiocarbon date (A13437) of 1915±30 was obtained from the humus of the 4Ab3 horizon.

3.2. Micromorphological features

Ah horizons of both buried paleosols of site 1 section have similar fabric. Isotropic dark fine material forms granular aggregates; however most of these granules are deformed and welded into larger subangular blocks, which could include also coarse grains of volcanogenic minerals. The blocks have irregular shapes and rough surfaces (Fig. 6A). Such fabric is not typical for the natural Andosols where the granular structure is better developed and inter-granular porosity is much higher. We observed compaction, due to deformation and welding of granules in some Andosols, strongly affected by humans. The matrix of 3A contains less dark organic pigment, than in 2Ah. Only in this horizon we observed a few large irregular fragments of brown clayey material with speckled b-fabric (Fig. 6B), similar to the matrix of the Bt and BC horizons of the nearby Acrisols at profile site 2. Taking into account that these fragments are absent in the paleosol parent rock and other genetic horizons as well as the size and shape of the fragments, we suppose that they are human-induced (probably a clayey

substance from Acrisols was used for construction or for ceramic production).

In the coarse material from the upper and middle parts of the polycyclic site 2 profile, we found two components of different origins: coarse grains of volcanogenic minerals and rocks and shale weathered fragments, with a clayey matrix with rounded quartz grains. We did not find large shale fragments in the surface soil, (which has only some tiny flakes of shale-derived clay), however, they are frequent already in the 2Ab1 horizon and abundant below. On the contrary, volcanogenic components with depth become fewer and more weathered; however they appear in minor quantities even in the b3 subprofile (Fig. 6C). Fine material is dominated by clay, likely originated from weathered shale. From the 2BCb1 horizon downwards, we observed voids with illuvial clay coatings. Coatings are rather few, thin, and without lamination (Fig. 6D). They are sometimes deformed and incorporated in the groundmass.

3.3. Soil physical and chemical characteristics

In the site 1 paleosols, PCh1 and PCh2 show similar grain size distributions. Sand fractions reach more than 75% (Fig. 7A). Clay content is very low, especially in the parent material of both soils; however, in PCh2, it increases in the B horizon, with a difference of 15% in comparison with the underlying horizon. The B horizon of PCh1 also shows an increment, but it is lower (7%).

Differences are found in site 2. In this case, PCh1 is also sandy with low quantities of clay, but a little bit higher than in site 1. PCh2 is more clayey, reaching more than 40% of clay, but having an increase of 15% showed by this soil in site 1. PCh3 is also very clayey but it does not have a clay accumulation in any part of the soil; all its horizons have similar clay contents of around 50%. The modern soil developed on the 1982 eruption tephra is sandy in the study sites (>75% of sand).

Values of Fe extracted by an oxalate solution (Feo) in all studied soils are very similar, varying from 4 to 12 mg/g. The lowest values correspond to PCh3 and the highest to PCh2 in site 2 (Fig. 7A). Fe extracted with DCB (Fed) exhibits some differences. The lowest content of Fe appears in PCh1 of both sites, even lower than in the modern soil. PCh2 has slightly higher values in site 1 that increase in site 2 and are similar to those exhibited by PCh3. Alo (Al extracted by oxalate) has also the highest proportions in PCh2 in both sites, but the lowest values of Alp (Al extractable with pyrophosphate solution).

pH in NaF was obtained in order to establish Andic properties. Both, the modern soils in site 2 and near the crater have values of 8 to 8.9. PCh3 has 8.9 while all horizons of PCh1

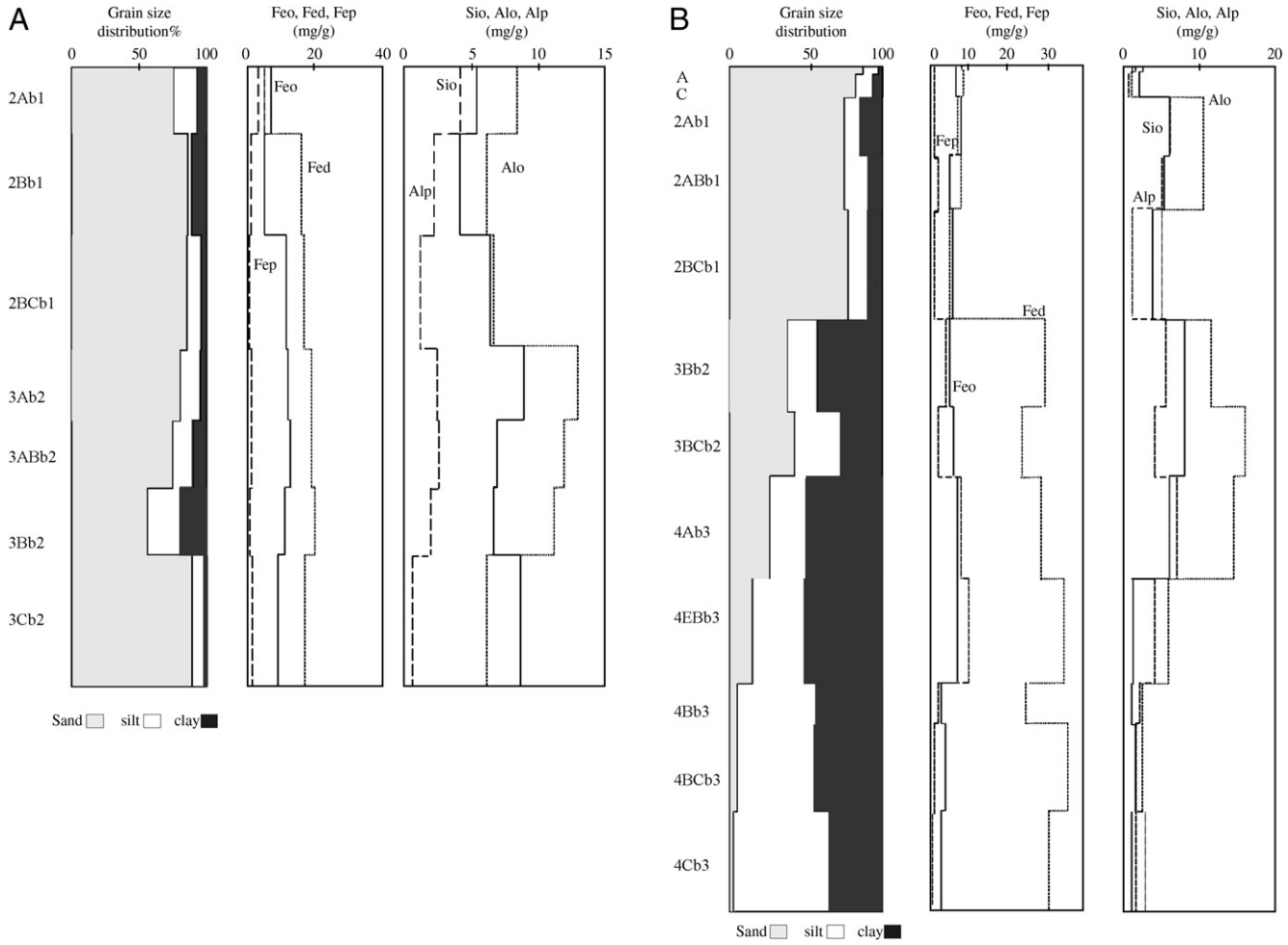

Fig. 7. Selected physical and chemical properties of study soils. A) PCh1 and PCh2 at site 1; B) PCh1, PCh2 and PCh3 at site 2.

and PCh2 have more than 9.5. These figures confirm the classification of these two paleosols as Andosols.

Organic carbon content is similar for A horizons of the modern soil and the PCh1 of the site 1 profile (Table 1). The lowest proportion corresponds to the 2Ab2 horizon of PCh2 (1.45%), while in 4Ab3 (PCh3) in site 2 profile reaches 3.7%.

Although there is a large difference in the organic carbon content in PCh1 and PCh2 in site 1, their C/N ratios are similar (Table 1). The values of $\delta^{13}C$ are also comparable, varying from −25.16 to −24.54, respectively (Table 1). The highest values of $\delta^{13}C$ were found in the modern soil and in the PCh3 in site 2 (−19.8).

3.4. Soil mineralogy

Fine sand fractions in the volcanic sediments of the El Chichón eruptions consist of minerals, typical for andesitic pyroclastic material: plagioclases, amphiboles, volcanic glass, fragments of effusive rocks, with minor amounts of pyroxenes and opaque grains. The proportions, however, vary among the sediments of different events: the 550 yr B.P. tephra is enriched in volcanic glass whereas 1250 yr B.P. tephra and especially that of the 1982 eruption (crater profile) contain more plagioclases and rock fragments. Besides, a higher quantity of biotite was detected in the 1250 yr B.P. sediment. The two buried soils of site 1 show a similar tendency of volcanic glass decrement in A horizons, compared to the parent materials (Fig. 8).

In site 2, the same volcanogenic minerals dominate in the upper and middle horizons. We observed differences in the component abundance among the strata: 2BC horizon, which we associated with the 550 yr B.P. fall, is enriched in volcanic glass, whereas C and 3BC horizons (attributed to 1982, and 1250 yr B.P. eruptions, respectively) have more plagioclases, and besides, 3BC has an elevated biotite content. Major changes in the composition of the fine sand fraction were detected in the 4BC horizon. Here, altered grains are more abundant with the appearance of muscovite and chlorite admixture, all of them likely originated from the underlying shales. However, even here, the components typical of pyroclastic material, plagioclase and volcanic glass, still account for more than 50% of the fine sand fraction.

The clay fraction from the Regosol A horizon, formed on the 1982 eruption tephra, has not produced any peaks of the crystalline clay components. Conspicuously enough, clear 14 Å maximum partly shifting to 16 Å in the ethylene glycol treated specimen and collapsing to 10 Å under heating appeared in the

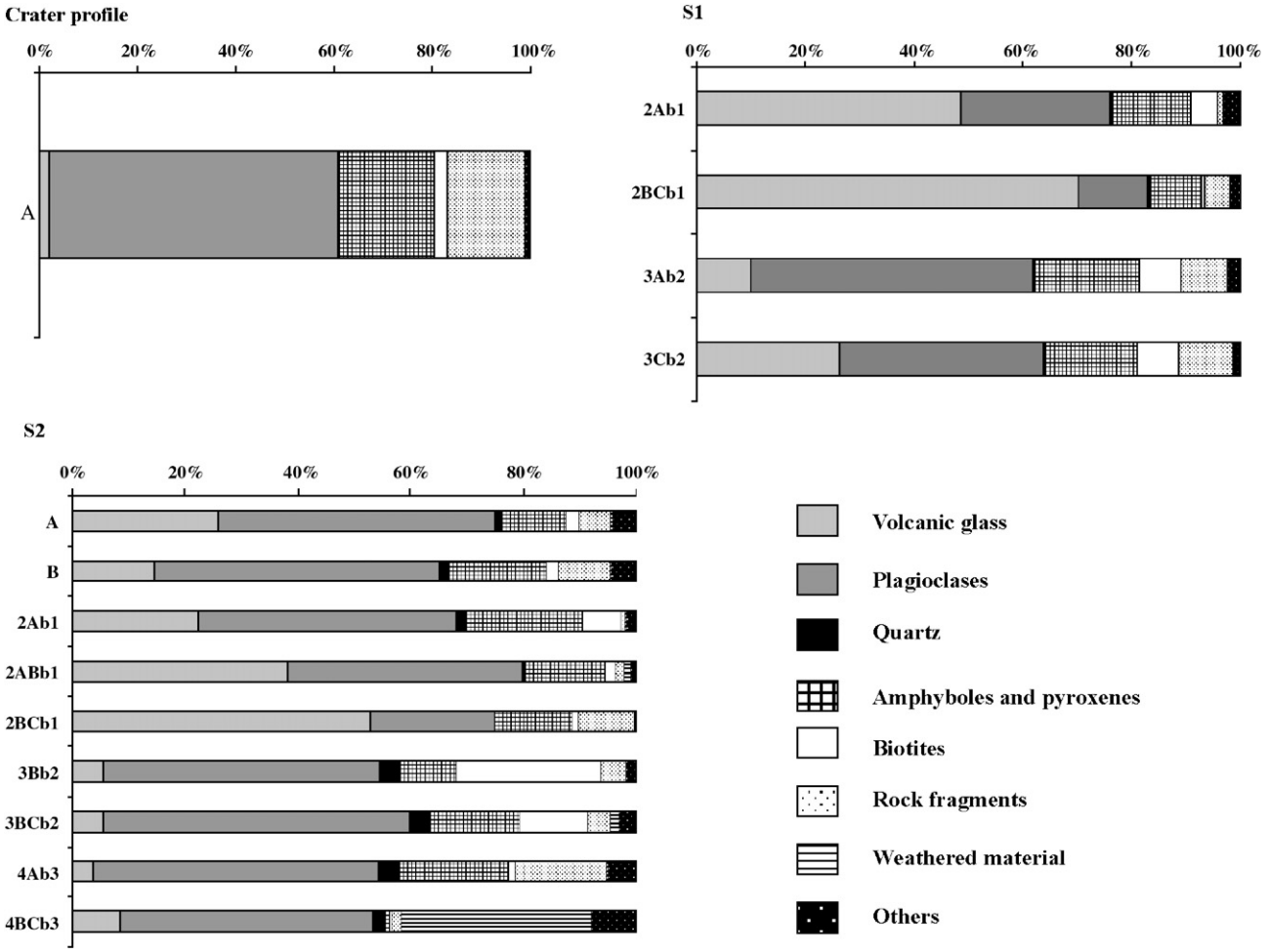

Fig. 8. Mineralogy of the fine sand fraction of selected horizons of the paleosols.

clay diffractogram of the C horizon sample. This pattern indicates the presence of vermiculite and smectite in the most recent pyroclastic sediments of El Chichón, as reported by Macías et al. (1997), although they have no morphological evidence of weathering and pedogenesis thus formed by hydrothermal activity.

The clay diffractograms of all horizons of the b1 and b2 paleosols in PCh1 do not demonstrate characteristic peaks of clay mineral crystals. A broad "hump" between 2θ 18° and 34° is evidence of the abundance of amorphous material.

Major differences among clay mineral assemblages of different horizons were detected within the polycyclic PCh2 (Table 2). The upper unit A–C is characterized by the presence of 14 Å components: vermiculite (no peak shifts on glycolation, and to 10 Å on heating) in the A horizon and smectite (peak shifts to 17 Å after ethylene glycol treatment) in the C horizon. Both these minerals were identified also in the 2Ab1 and (traces) in the 2BCb1 horizons of the second subprofile, however the latter did not show any evidence of crystalline clay. The specimens from the 3Bb2 and 3BCb2 horizons of the third subprofile, besides 14 Å minerals, contain illite (10 Å maximum, remaining unchanged after glycolation and heating).

Finally, major differences are observed in the mineral associations of the inferior b3 subprofile, developed on lutites. Diffractograms from this part of the sequence have sharper and higher diagnostic peaks of clay minerals than those of overlying units, indicative of their higher crystallinity. Vermiculite (14 Å) and illite (10 Å) are detected in the whole b3 horizon set, showing however the inverse pattern of profile distribution. Vermiculite content increases in the upper 4Ab3, 4EBb3 and 4Bb3 horizons, whereas illite is more abundant in BCb3 and Cb3. Besides 2:1 minerals, kaolinite was identified only in the b3 subprofile by its 7.2 Å maximum (Table 2). We discard the supposition that this maximum belongs to the vermiculite series (second order) because it persists after heating the sample to 400 °C whereas the first order 14 Å peak of vermiculite collapses to 10 Å.

Table 2
Mineralogy of the clay fraction

Soil, horizon	Amorphous	14 Å labile minerals (vermiculite, smectite)	Mica	Kaolinite
Profile crater				
AO	+			
C	+			
Profile S1				
2Ab1	+++			
2BCb1	++			
2Ab2	+++			
3Bb2	+++			
Profile S2				
A	+	++		
C	+	++		
2Ab1	+	++		
2ABb1	++	+		
2BCb1	++			
3Bb2		++		
3BCb2		++	++	
4Ab3		+++		++
4EBb3		+++	+	+++
4Bb3		++	+	+++
4BCb3		+	+++	++
4Cb3		++	+++	++

+: scarce.
++: present.
+++: abundant.

4. Discussion

4.1. Andosols on the 550 yr B.P. and 1250 yr B.P. tephras: are paleoenvironmental inferences possible?

Soil development on the 1982 eruption deposits is very poor and resulted in the formation of a weak Regosol. On the contrary, soils on tephras from two earlier volcanic events are well developed Andosols with A–B–C profiles. We supposed that "memory" of these profiles could contribute in reconstructing the environmental change recorded during the last 1200 yr in humid tropics of Mesoamerica that still has not been sufficiently documented.

Two buried soils of profile site 1 display clear differences of the properties of the A horizons. In the PCh1, the A horizon is thinner, but darker, with well developed granular structure; it has a lower reflectance (13.25%) and a higher OC content (3.61%). The A horizon of the PCh2 is thicker but paler, the structure is subangular blocky and the reflectance is higher both in dry and moist samples (16.65–7.8%, respectively), that correlates with lower values of OC (1.45%). To interpret these differences one should take into account soil forming factors such as: geomorphologic position, parent material (andesitic tephra) and duration of pedogenesis (that in this case do not differ significantly for the two buried paleosols). These can be explained either by a change in the bioclimatic conditions (climate and vegetation) or by differences in the type and intensity of human impact on soils.

First, we associated the lower humus content and correlated morphological properties of PCh2-A horizon on the 1250 yr B.P. tephra with a drier paleoclimate. This seemed to be in good agreement with recent studies that claimed a pronounced dry period in tropical Mesoamerica during the end of the first millennium A.D., which is proposed as a major reason for the rapid decline of the Maya civilization (Haug et al., 2003), as well as with lacustrine records in the Tuxtlas area (Lozano-García and Caballero-Miranda, 2004), near San Martin volcano (Fig. 1). However, Espíndola et al. (2000) have concluded that the western Maya lowlands were more affected by eruptions of El Chichón that could have played an important role in the development of the environmental conditions that caused major droughts in the Yucatan peninsula.

On the other hand, a number of earlier studies on modern Andosol climosequences have shown a tendency that higher humus accumulation accompanies the increase of humidity (Quantin, 1985; Miehlich, 1991).

In fact, other soil properties contradict our previous interpretation, concerning a drier climate in the area. First, the clay fraction in both paleosols (Table 2) is dominated by amorphous

components formed due to weathering of volcanic glass. The content of the crystalline clay minerals is below the detection limit of the X-ray diffraction method. The PCh2 paleosol has an even higher content of oxalate-extractable Si and Al, indicating a larger accumulation of allophane. This process is more typical for young volcanic soils formed in humid environments, whereas drier conditions result in rapid crystallization of amorphous compounds to halloysite (Parfitt and Wilson, 1985; Dubroeucq et al., 1998).

Second, the $\delta^{13}C$ values in the organic matter of both PCh1 and PCh2 paleosols are similar and rather low (Table 1). These values are indicative of a paleovegetation dominated by C3 plants and therefore points to soil development in humid forest ecosystems. In case of pronounced drying of this region, one should expect an invasion of C4 grasses and/or succulents of the CAM group (cactacea) with heavier C isotope composition of the biomass, with the consequent increase of $\delta^{13}C$ in humus.

Thus mineralogy and stable C isotope composition, which earlier proved to be rather sensitive indicators of wet/dry oscillations in volcanic paleosols (Sedov et al., 2003b), did not support the hypothesis of more arid pedogenesis for the PCh2 paleosol. Both Andosols formed on the 550 yr B.P. and 1250 yr B.P. tephras correspond to humid climatic conditions, like those prevailing at present. The differences in the humus content between them can be interpreted in another way. The lower PCh2 paleosol has evidences of ancient human impact, in particular numerous ceramic fragments, also shown in thin sections (Fig. 6B). It is likely to be affected by diverse human activities, during the Late Classic/Postclassic period, such as agriculture, urban development and deforestation that caused soil compaction and decreased humus content. In fact, Espíndola and co-workers (2000) found a lot of home-made ceramics, indicating that the area was settle for at least 2400 years.

Actual forest cleaning and cultivation of Andosols in the humid tropics is known to result in a rapid loss of humus accompanied by changes in structure and porosity (Geissert et al., 2000). Guo and Gifford (2002) estimated a world average soil organic carbon (SOC) loss of 49% and 58% after conversion of native forest to pastures and crops, respectively. Although, Parfitt et al. (1997) considered that a large part of the organic matter in Andosols is complexed with short-range ordered minerals, the SOC content declines little with cropping. The differences in Alo and Alp contents between the two buried paleosols could also be explained in the framework of the hypothesis of the differentiated human impact. Both allophanes (evaluated by Alo and Sio) and Al-organic complexes (evaluated by Alp) are the main pedogenic components formed in humid Andosols, where Al is liberated by weathering. However, the relation between these components is related to the quantity and quality of organic components, entering the soil system, and is not necessarily climate-dependent, as Matus et al. (2006) showed in a study of Chilean volcanic soils. We suppose that the lower paleosol PCh2 experienced more prolonged and profound human impact, implying not only cultivation, but also household activities. This implies deeper perturbation of soil and destruction of vegetation cover, with consequent decline of the plant residues input. As a consequence, in the lower paleosol the formation of Al-organic compounds was suppressed and allophanes became dominant, whereas in the upper paleosol PChl having less dramatic anthropogenic perturbation, Al-organic complexes are more abundant.

Then, we attribute differences in SOM content due to strong human impact on soil cover which is in agreement with several studies in different parts of the Maya region (Beach, 1998; Beach et al., 2003; among others).

The dry episode recorded in the Late Classic–Postclassic Maya period, if it occurred in the El Chichón area, was too short to be recorded in the soil memory (below the resolution of the paleopedological record). Supposing it could be an event (or set of events) which took place at a yearly to decadal scale, its effect in the economic and cultural development of Mayas should be viewed in terms of superimposing of climatic fluctuations over long-term landscape transformation by humans.

4.2. Two-storied profile of Andic Acrisol: differentiation controlled by parent material and duration of pedogenesis.

Profile site 2 demonstrates contrasting differences between properties of the upper set of horizons: A–C–2(Ab1–ABb1–BCb1)–3(Bb2–BCb2) and the lower b3 subprofile, which represents the superpositioning of two pedogenic events, operating in different parent materials, on different time scales.

In fact, the upper set constitutes a pedocomplex, developed in the same sequence of pyroclastic sediments: 1982, 550 yr B.P. and 1250 yr B.P. eruptions, exposed in the crater and site 1 profiles. Thus we correlate the b1 subprofile with PCh1 and b2 subprofile with PCh2. This is supported by stratigraphic position and morphology of tephra horizons: C, 2BCb1 and 3BCb2, and confirmed by the mineralogical composition of the sand fractions. This correlation allows attributing the origin of the 14 Å minerals in the upper part of this set, to hydrothermal processes, as described for the crater profile. However, in site 2, these sediments did not achieve sufficient thickness to separate individual soils, formed on them, nor to bury the older b3 subprofile (PCh3 paleosol) deep enough to isolate it from actual pedogenesis.

In this set, we detect a typical assemblage of rapid pedogenetic processes, known to develop in the young volcanic sediments under humid climate: moderate weathering of unstable primary minerals, especially volcanic glass, accompanied by precipitation of short-range order components, mostly allophanes; accumulation of humus, bound to allophanes; development of fine granular structure, providing high porosity of the solum. These processes are reflected by morphological properties as well as analytical characteristics: relatively small clay content, but high quantities of oxalate-extractable Al, Si, Fe, and elevated OC values (Table 1, Fig. 7B). The set of processes and properties in this unit corresponds to Andosol pedogenesis.

The radiocarbon date, 1915 ± 30 yr B.P., of the 4A horizon is indicative of the minimum age of the inferior b3 subprofile (Matthews, 1985). Its pedogenesis is supposed to develop mostly from shales, rich in phyllosilicates, although the addition of some pyroclastic material older than 1900 yr B.P. in its upper part is possible as attested by the stratigraphic record of El

Chichón (Espíndola et al., 2000). This possibility is supported by the increase of sand content in the 4Ab3 and 4Eb3 horizons, together with the fact that this fraction consists mostly of volcanic minerals.

Contrary to the overlying unit, here we identify a set of processes of advanced humid tropical pedogenesis and weathering which are supposed to operate over longer periods, among them: destruction of a large portion of primary minerals and accumulation of fine alteration products, so that the clay fraction exceeds 40% of the soil mass; synthesis of iron oxide and kaolinite, typical components of ferrallitic weathering crusts, confirmed by maximal values of dithionite-extractable iron (Fed) together with low Feo/Fed ratio, and by X-ray diffraction patterns of clay fractions; degradational transformation of micas towards labile 2:1 minerals — vermiculite and smectite documented by inverse profile distribution of vermiculite (maximum in upper horizons were weathering is more active) and illite (maximum in the bottom of the subprofile); moderate clay illuviation, reflected in clay cutans in the 4Bb3 horizon. The processes and features of the b4 subprofile demonstrate the tendency of the pedogenesis towards Acrisol formation.

The boundary between "young Andosolic" and "old Acrisolic" subprofiles is diffuse. Illite — the marker of the shale-derived material is detected already in the b2 subprofile, whereas volcanic minerals in the sand fractions are abundant down to the 4BCb3 horizon. We attribute this "overlapping" to the biopedoturbation and to the colluviation, which is likely to accompany sedimentation of the pyroclastic materials.

The set of soil forming processes detected in both "stories" of this soil corresponds to humid forest ecosystems, which was predominant over a much longer period, than the Late Holocene. However, somewhat higher values of $\delta^{13}C$ of humus in the 4Ab3 horizon (Table 1) could be indicative of the presence of C4 plants in the vegetation cover during the end of the formation period of the b3-PCh3 subprofile (humus in the buried soils is representative of the final stages of their pedogenesis — see Matthews, 1985). Taking into account the 14C age of b3 humus, it allows us to suppose a short-term drier stage about 2000 yr B.P., not at the end, but rather at the beginning of the Classic Mayan period.

Although the information about such two-storied profiles is still scarce, they could be rather frequent in the periphery of the areas of volcanic activity, located in or neighboring to the humid (sub)tropical regions. A similar case of a thin Andosol developed over a highly weathered polycyclic Luvisol was reported by Solleiro-Rebolledo et al. (2003) in the Glacis de Buenavista, Morelos State. O. Ascanio (personal communication, 2005) informed us about "strange" Acrisols with thick dark humus horizons (most probably containing recent pyroclastic material) near Córdoba, Veracruz state. Both sites are located at the boundaries of the Trans-Mexican Volcanic Belt, characterized by high eruptive activity throughout Late Quaternary.

Acknowledgments

This work was supported by CONACYT grant 38586-T to J.-L. Macías. We thank E. Lounejeva, E. Cienfuegos and P. Morales who carried out stable isotope analyses. K. Shimada and L. Mora for total organic carbon and nitrogen determination; A. González for physical and chemical determinations; L. Flores for colorimetric analyses; H. Cabadas for quantification of sand mineralogy; and H. Rueda who made the digital model of El Chichón volcano. We appreciate the reviews made by A. Makeev and O. Chadwick that improved the manuscript.

References

Beach, T., 1998. Soil catenas, tropical deforestation, and ancient and contemporary soil erosion in the Petén, Guatemala. Physical Geography 19, 378–405.

Beach, T., Dunning, N., Luzzadder-Beach, S., Scarborough, V., 2003. Depression soils in the lowland tropics of Northwestern Belize: anthropogenic and natural origins. In: Gómez-Pompa, A., Allen, M., Fedick, S., Jiménez-Orsonio, J. (Eds.), The lowland Maya Area: Three Millennia at the Human-Wildland Interface. Haworth Press, Binghampton, NY, pp. 139–174.

Campbell, I.B., 1986. Recognition of paleosols in Quaternary periglacial and volcanic environments in New Zealand. In: Wright, P.V. (Ed.), Paleosols: Their Recognition and Interpretation. Blackwell, London, pp. 208–240.

Canul, R.F., Rocha, V.L., 1981. Informe geológico de la zona geotérmica de "El Chichonal", Chiapas: Comisión Federal de Elctricidad, Morelia, Michoacán, México. 38 pp.

Damon, P., Montesinos, E., 1978. Late Cenozoic volcanism and metallogenesis over an active Benioff Zone in Chiapas, Mexico. Arizona Geological Society Digest 11, 155–168.

Dubroeucq, D., Geissert, D., Quantin, P., 1998. Weathering and soil forming processes under semi-arid conditions in two Mexican volcanic ash soils. Geoderma 86, 99–122.

Espíndola, J.M., Macías, J.L., Tilling, R.I., Sheridan, M.F, 2000. Volcanic history of El Chichón volcano (Chiapas, Mexico) during the Holocene, and its impact on human activity. Bulletin of Volcanology 62, 90–104.

Frezzotti, M., Narcisi, B., 1996. Late Quaternary tephra derived paleosols in central Italy's carbonate Apennine Range: stratigraphical and paleoclimatological implications. In: Lowe, D.J. (Ed.), Tephra, loess, paleosols — an integration. Quaternary International, vol. 34–36, pp. 147–153.

García-Palomo, A., Macías, J.L., Espíndola, J.M., 2004. Strike-slip faults and K-alkaline volcanism at El Chichón volcano, southern Mexico. Journal of Volcanology and Geothermal Research 136, 247–268.

Geissert, K.D., Ramírez Salazar, M., Meza Pérez, E., 2000. Propiedades físicas y químicas de un suelo volcánico bajo bosque y cultivo en Veracruz, México. Foresta Veracruzana 2 (1), 31–34.

Gill B.G., 1994. The great Maya droughts. PhD dissertation. Univ. Texas at Austin, 528 pp.

Guo, L.B., Gifford, R.M., 2002. Soil carbon stocks and land use change: a meta analysis. Global Change Biology 8, 345–360.

Haug, G.H., Günter, D., Peterson, L.C., Sigman, D.M., Hughen, K.A., Aeschlimann, B., 2003. Climate and the collapse of Maya civilization. Science 299, 1731–1735.

Jongmans A.G., 1994. Aspects of mineral transformation during weathering of volcanic materials: the microscopic and submicroscopic level. Thesis Wageningen, 143 pp.

Jongmans, A.G., Veldkamp, A., van Breemen, N., Staritsky, I., 1993. Micromorphological characterization and microchemical quantification of weathering in an alkali basalt pebble. Soil Science Society of America Journal 57, 128–134.

Lozano-García, S., Caballero-Miranda, M., 2004. Historia ambiental del Holoceno Tardío en la región de los Tuxtlas, Veracruz. IV Reunión Nacional de Ciencias de la Tierrab.

Macías, J.L., Sheridan, M.F., Espíndola, J.M., 1997. Reappraisal of the 1982 eruption of El Chichón volcano, Chiapas, Mexico: new data from proximal deposits. Bulletin of Volcanology 58, 459–471.

Macías, J.L., Arce, J.L., Mora, J.C., Espíndola, J.M., Saucedo, R., 2003. A 550-year-old Plinian eruption at El Chichon volcano, Chiapas, Mexico: explosive volcanism linked to reheating of the magma reservoir. Journal of Geophysical Research 108 (B12,2569), 3–18.

Matthews, J., 1985. Radiocarbon dating of surface and buried soils: principles, problems and prospects. In: Richards, K., Arlett, R., Ellis, S. (Eds.), Geomorphology and Soils. Allen & Unwin, London, pp. 271–288.

Matus, F., Amigo, X., Kristiansen, S.M., 2006. Aluminium stabilization controls organic carbon levels in Chilean volcanic soils. Geoderma 132, 158–168.

Miehlich, G., 1991. Chronosequences of volcanic ash soils. Hamburger Bodenkundliche Arbeiten, vol. 15. Hamburg.

Mook, W.G., Jongsma, J., 1987. Measurement of the N_2O corrections for 13C/12C ratios of atmospheric CO_2 by removal of N_2O. Tellus 39B, 96–99.

Munsell Soil Color Charts, 2000. Macbeth Division of Kollmorgen Corporation, Baltimore, Maryland. Revised washable edition.

Parfitt, R.L., Wilson, A.D., 1985. Estimation of allophane and halloysite in three sequences of volcanic soils, New Zealand. In: Fernández-Caldas, E., Yaalon, D.H. (Eds.), Volcanic Soils. Weathering and landscape relationships of soils on tephra and basalt. Catena Supplement, vol. 7, pp. 1–8.

Parfitt, R.L., Theng, B.K.G., Whitton, J.S., Shepherd, T.G., 1997. Effects of clay minerals and land use on organic matter pools. Geoderma 75, 1–12.

Quantin, P., 1985. Characteristics of the Vanuatu Andosols. In: Fernandez-Caldas, E., Yaalon, D.Y. (Eds.), Volcanic Soils. Catena Supplement, vol. 7, pp. 99–105. Braunschweig.

Sedov, S., Solleiro-Rebolledo, E., Gama-Castro, J., Vallejo-Gómez, E., González-Velázquez, A., 2001. Buried Paleosols of the Nevado de Toluca: an alternative record of Late Quaternary environmental change in central Mexico. Journal of Quaternary Science 16 (4), 375–389.

Sedov, S., Solleiro-Rebolledo, E., Gama-Castro, J., 2003a. Andosol to Luvisol evolution in central Mexico: timing, mechanisms and environmental setting. Catena 54, 495–513.

Sedov, S., Solleiro-Rebolledo, E., Morales-Puente, P., Arias-Herrería, A., Vallejo-Gómez, E., Jasso-Castañeda, C., 2003b. Mineral and organic components of the buried paleosols of the Nevado de Toluca/central Mexico as indicators of paleoenvironments and soil evolution. Quaternary International 106–107, 169–184.

Shoji, S., Nanzyo, M., Dahlgren, R., 1993. Volcanic ash soils: genesis, properties and utilization. Developments in Soil Science, vol. 21. Elsevier, Amsterdam.

Sigurdsson, H., Carey, S.N., Espíndola, J.M., 1984. The 1982 eruptions of El Chichón volcano, Mexico: stratigraphy of pyroclastic deposits. Journal of Volcanological Research 23, 11–37.

Sofer, Z., 1980. Preparation of carbon dioxide for stable carbon isotope analysis of petroleum fractions. Analytical Chemistry 52, 1389–1391.

Solleiro-Rebolledo, E., Sedov, S., Gama-Castro, J.E., Flores-Román, D., Escamilla-Sarabia, G., 2003. Paleosol-sedimentary sequences of the Glacis de Buenavista, central Mexico: interaction of Late Quaternary pedogenesis and volcanic sedimentation. Quaternary International 106–107, 184–201.

Targulian, V.O., Goryachkin, S.V., 2004. Soil memory: types of record, carriers, hierarchy and diversity. Revista Mexicana de Ciencias Geológicas 21, 1–8.

Ugolini, F.C., Dahlgren, R.A., 2002. Soil development in volcanic ash. Global Environmental Research 6, 69–81.

USDA. 1996. Soil Survey Laboratory Methods Manual. Soil Survey Investigations Report No. 42. U. S. Department of Agriculture, National Resources Conservation Services, National Soil Survey Center.

Wada, K., 1985. The distinctive properties of Andosols. In: Steward, B.A. (Ed.), Advances in Soil Science, vol. 2. Springer, New York, pp. 173–229.